

GIANA Polyp Segmentation with Fully Convolutional Dilation Neural Networks

Yun Bo Guo and Bogdan J. Matuszewski^a

*Computer Vision and Machine Learning (CVML), Research Group, School of Engineering,
University of Central Lancashire, Preston, U.K.*

Keywords: Fully Convolutional Neural Networks, Dilation Convolution, Polyp Segmentation, Video Colonoscopy, Segmentation Quality.

Abstract: Polyp detection and segmentation in colonoscopy images plays an important role in early detection of colorectal cancer. The paper describes methodology adopted for the EndoVisSub2017/2018 Gastrointestinal Image ANALysis – (GIANA) polyp segmentation sub-challenges. The developed segmentation algorithms are based on the fully convolutional neural network (FCNN) model. Two novel variants of the FCNN have been investigated, implemented and evaluated. The first one, combines the deep residual network and the dilation kernel layers within the fully convolutional network framework. The second proposed architecture is based on the U-net network augmented by the dilation kernels and “squeeze and extraction” units. The proposed architectures have been evaluated against the well-known FCN8 model. The paper describes the adopted evaluation metrics and presents the results on the GIANA dataset. The proposed methods produced competitive results, securing the first place for the SD and HD image segmentation tasks at the 2017 GIANA challenge and the second place for the SD images at the 2018 GIANA challenge.


1 INTRODUCTION

Colorectal cancer is one of the leading causes of cancer deaths worldwide. Often, it arises from benign polyps which with time become malignant. To decrease mortality, an early detection and assessment of polyps is essential. For an initial evaluation, an image of a segmented polyp could provide important evidence to describe polyp characteristics. In the current routine clinical practice, polyps are detected and delineated in colonoscopy images manually by highly trained clinicians. To automate these processes, machine learning and computer vision techniques have been considered to improve polyps’ detectability and segmentation objectivity (Bernal et al., 2015).

An automatic polyp segmentation is a very challenging task. This is because polyps’ appearance, shape and size are highly variable (see Figure 1). In the early stages, a colorectal polyp is small and could have no obvious differentiating texture appearance, and therefore could be easily confused with other intestinal tissue. In the later stages polyps

progressively change, often significantly increasing in size and could develop more distinctive texture and colour patterns. Some of the polyps grow so large, that they will take most of the camera field of view, possibly not fitting entirely into the image frame. Additionally, illumination used in the colon screening can cause image artefacts, with pattern of shadows, highlights and occlusions, making the segmentation task even harder. A single polyp could look significantly different depending on the camera position. Furthermore, for some polyp types there is no apparent boundary between the polyp and the surrounding tissue. As in most cases of manual delineation, polyp segmentation is affected by the lab’s guidelines and experience of the clinician. It is therefore hard to determine the gold standard for the automatic segmentation procedures dealing with all possible types of polyps.

This paper proposes novel fully convolutional neural networks to accomplish this challenging segmentation task. The FCNN methods that were developed produce the polyp occurrence confidence map (POCM). The polyp position in the image frame

^a <https://orcid.org/0000-0001-7195-2509>

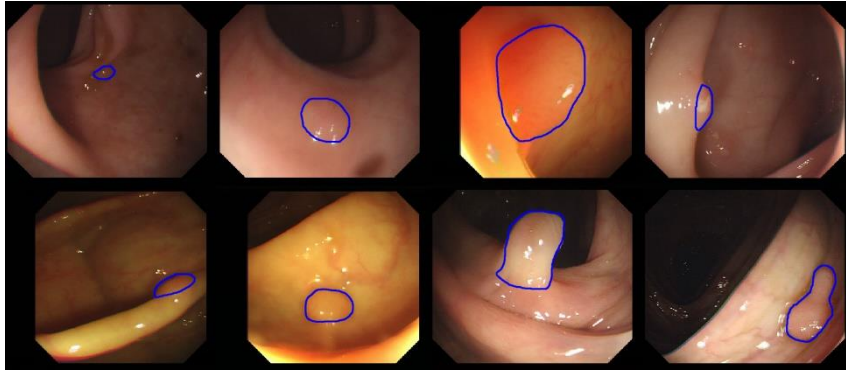


Figure 1: Examples, from the GIANA SD training dataset, showing polyps with different size, position, shape and colour. The blue contour is the ground truth marked by clinicians.

is indicated by higher values of the POCM. In the post-processing, the final polyp delineation is either obtained by simple thresholding or the hybrid-level set (Zhang et al. 2008, 2009) is used on the POCM to smooth the polyp contour and eliminate small noisy network responses.

2 RELATED WORK

Most of the existing polyp segmentation methods can be divided into two main approaches based either on polyp apparent edge or texture. Due to the fact that in many cases, polyps have well-defined shapes, some of the early approaches attempted to fit predefined polyp shape models. Hwang et al. (2007) used ellipse fitting techniques based on image curvature, edge distance and intensity values. Gross et al. (2009) used the Canny edge detector to process prior-filtered images, identifying the relevant edges using a template matching technique. Breier et al. (2011a, 2011b) investigated applications of active contours for the polyp segmentation. Although these methods perform well for typical polyps, they require manual contour initialisation.

The above mentioned techniques rely heavily on a presence of complete polyp contours. To improve the robustness, further research was focused on the development of robust edge detectors. Bernal et al. (2012) presented a “depth of valley” concept to detect more general polyp shapes, then segment the polyp through evaluating the relationship between the pixels and detected contour. Further improvements of this technique are described in (Bernal et al., 2013) and (Bernal et al., 2015). In the subsequent work, Tajbakhsh et al. (2013) put forward a series of polyp segmentation method based on edge classification, utilising the random forest classifier and Haar

descriptor features. In the follow-up work (Tajbakhsh et al. 2014a, 2014b) segmentation was refined via use of several sub-classifiers.

Another class of polyp segmentation methods is based on texture descriptors, typically operating on a sliding window. Karkanis et al. (2003) combined Grey-Level Co-occurrence Matrix (GLCM) and wavelet. Using the same database and classifier, (Iakovidis et al., 2005) proposed a method which provided the best results in terms of area under the curve (AUC) metric. Local Binary Pattern and the original GLCMs methods are also tested in (Alexandre et al. 2008), however, because of a different dataset, and values of the design parameters, the results cannot be directly compared. More recently, with advances in deep learning, hand-crafted feature descriptors are gradually being replaced by convolutional neural networks (CNN) (LeCun et al. 1998) and (Krizhevsky et al. 2012).

Park et al. (2015) formulated a pyramid CNN to learn the scale-invariant polyps’ features. The features are extracted from the same patch at three different scales through three CNN paths. Ribeiro et al. (2016) evaluated CNN comparing it with other state-of-art hand-crafted features used for polyp classification, and found that CNN has superior performance. CNN is not only used for recognition but also for feature extraction. R. Zhang et al. (2017) designed a transfer learning scheme. They used a pre-trained CNN to extract low-level polyp features and SVM for classification. It illustrates that CNN can learn informative and robust low-level features.

However, the general problem with the sliding window approach is that it is harder to use image contextual information and it is inefficient in the prediction mode (i.e. segmentation of the test images). This problem has been addressed by the so called fully convolutional networks (FCN), with the

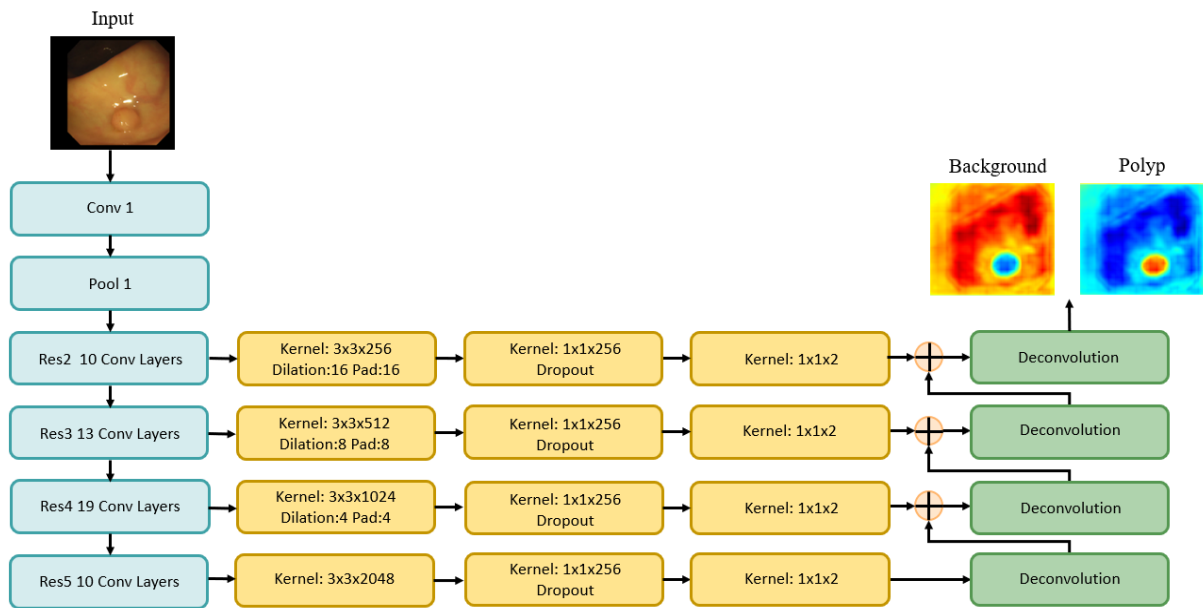


Figure 2: The proposed Dilated ResFCN polyp segmentation network. From left to right, Blue: Feature extraction part; Yellow: Dilation convolution; Green: Skip connection.

two key architectures (Long et al. 2015) and (Ronneberger et al., 2015). These methods can be trained end-to-end and output complete segmentation results, without a need for any post-processing. Vázquez et al. (2017) and Akbari et al. (2018) directly segmented the polyp image by standard FCN. L. Zhang et al. (2017) use the same FCN, but they add a random forest to decrease the false positive. The U-net (Ronneberger et al., 2015) is one of the most popular architectures for biomedical image segmentation. It has been also used for polyp segmentation. Li et al. (2017) designed a U-net architecture for polyp segmentation with smooth contours.

In recent years, it has been noticed that there is a close relationship between receptive fields and segmentation results of convolutional networks. As for generic image segmentation, a new layer called dilation convolution has been proposed (Yu et al. 2015) to control the CNN receptive field in a more flexible way. Chen et al. (2018) also utilised dilation convolution and developed further network changes called atrous spatial pyramid pooling (ASPP) to learn the multi-scale features. The ASPP module consists of four parallel convolutional layers with different dilations.

In summary, polyp segmentation is becoming more and more automated and integrated. Deep feature learning and end-to-end architectures are gradually replacing the hand-crafted features operating on a sliding window. Polyp segmentation can be seen as a

semantic instance segmentation problem and therefore, a large number of techniques developed in computer vision for generic semantic segmentation could possibly be adopted, providing effective and more accurate methods for polyp segmentation.

3 METHOD

3.1 Pre-processing

The first step in the proposed processing pipeline is the removal of black borders in the images. The border pixels have small random intensity variations, and therefore CNN could be “distracted” and learn unnecessary image border patterns. It has been found that the border pixels obtained from the same video sequence have always the same value. After video sequence detection, images from the same video are stacked and the border can be easily located via analysis of local variance. To save the memory and training computational load, all the input images are re-scaled to 250x287x3 in size.

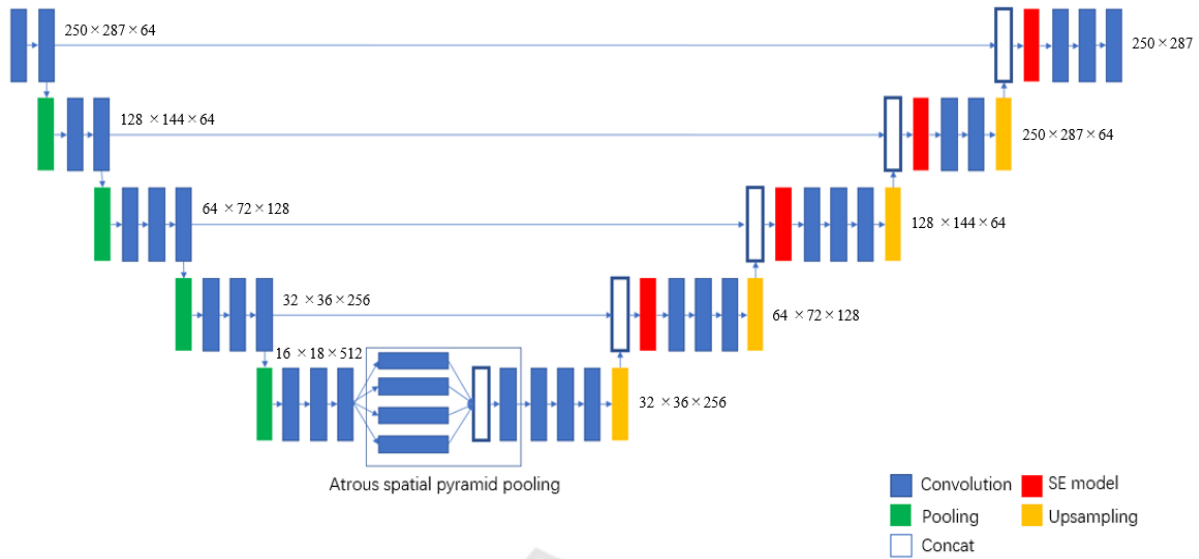


Figure 3: The structure of the proposed SE-Unet architecture.

3.2 Dilated ResFCN

The first proposed network architecture, Dilated ResFCN, is shown in Figure 2. It is derived from the architecture proposed by (Peng et al., 2017). The proposed network consists of three sub-structures performing different tasks, these are: feature extraction layers, multi-resolution classification layers and the deconvolution layers. The feature extraction part of the network is based on the previously proposed ResNet50 model (He et al. 2016). It can be divided into five sub components. Res1 – Res5. The Res1 represents the first convolutional and pooling layers. Res2 – Res5 represents the sub-networks having respectively 9, 12, 18, 9 convolutional layers with 256, 512, 1024, 2048 feature maps. Each of these sub-networks operates on the gradually spatially reduced feature maps, down-sampled with a stride of 2 when moving from sub-network Res i to the sub-network Res $i+1$, the size of corresponding feature map is 62×72 , 31×36 , 16×18 , 8×9 . Excluding the regular connection, the outputs from the Res2 to Res5 is being directed to parallel classification paths consisting of a dilation convolutional layer, 1×1 convolutional layer, dropout layer and final 1×1 convolutional layer with two outputs corresponding to the polyp and background confidence maps. There are four such parallel paths fed from the outputs of Res2- Res5, with each path

using different dilations. The outputs of these four paths are subsequently combined by skip connection which includes the deconvolution layers and fusion layer.

In the proposed Dilated ResFCN network, the deconvolution layers perform bilinear interpolation without training. The initial weights of the proposed architecture have two sources: The feature extraction part is initialized by a publicly available ResNet-50 model, which was trained on the ImageNet. The convolutional layers in the four parallel paths are initialized by the Xavier method (Glorot and Bengio, 2010). The network is trained with softmax cross-entropy loss using Adam optimizer.

3.3 SE-Unet

The second proposed network, SE-Unet, is shown in Figure 3. It is design to segment polyps which have been missed by the ResFCN as it more “sensitive” in some cases than ResFCN, however overall tends to produce more false positive pixels. This method is inspired by the U-net and SE-net (Hu et al., 2017). The whole network can be divided into four parts, consisting of feature learning, up-sampling, Atrous spatial pyramid pooling (ASPP) and SE-modules.

The VGG16 network is used as an encoder with the decoder being a mirrored VGG16. The resolution of the last encoder layer is 16×18 . The ASPP is used to learn the multi-scale high-level features, it consists of

1×1 kernel, 3×3 kernel, and two dilation kernels with dilation rates 2 and 4. Each component of ASPP outputs 256 feature maps, so the total number of feature maps is 1024.

Pixels at the same position are fused by a 1×1×256 kernel. The SE-module is added behind each concatenation layer in the up-sampling module. For each feature map in the concatenation layer it assigns a coefficient between zero and one. Large coefficients indicate that the corresponding features have more significance.

The up-sampling layers implement bilinear interpolation and the initial weights are selected using the Xavier method. The network is trained with the sigmoid cross-entropy loss using Adam optimizer.

4 IMPLEMENTATION

4.1 Dataset

The proposed polyp segmentation methods are developed and evaluated on the database from the EndoVisSub2017 GIANA Polyp Segmentation Challenge. The training database, with the ground truth segmented polyps, has two subsets: (i) SD (CVC-ColonDB), consisting of 300 low resolution 500-by-574 pixels polyp images, and (ii) HD, with 56 high resolution 1080-by-1920 pixels images. The test database has 612 SD (CVC-ClinicDB) images with reduced 384-by-288 resolution and 108 full resolution HD images. For selection of the methods' design parameters, 4-fold tests have been performed on the training data. The SD subset consist of the images extracted from a few video sequences, with images from the same sequence being highly correlated (i.e. showing the same polyp). Therefore, when constructing the validation data folds, care was taken not to include any images from the same video simultaneously in the training and test subsets for any of the folds. This paper only reports the results obtained for the SD images.

4.2 Data Augmentation

Data augmentation is a standard technique, used to enlarge training data sets. It is frequently used, particularly in cases when the available dataset is relatively small. More recently, it has been reported that data augmentation can play an important role in controlling the generalisation properties of deep networks, e.g. Hernández and König (2018) has experimentally demonstrated that the augmentation alone could provide better results on test data, than in

combination with the weight decay and dropout. Whereas the training data augmentation is now commonly accepted methodology, data augmentation during the test time is not yet extensively used. However it is gradually growing in popularity. It is anticipated that it can further improve generalisation properties of the deep architectures.

4.2.1 Training Data Augmentation

From a perspective of a typical training set used in a context of the deep learning, the training data available for the polyp segmentation (see section 4.1) is rather small. Therefore, available data were heavily augmented with random rotation, translation, scale changes as well as colour and contrast jitter. In total, after augmentation, the training data include more than 90,000 images. Based on ablation tests with the FCN8 and Dilated ResFCN networks, it has been concluded that rotation and colour jitter have the most significant effect on improvement of the segmentation performance. Although intuitively not necessary obvious, the colour jitter plays an important role. This can be explained by the fact that the network is trained on the data from a small number of subject and the original images don't reflect all possible variations of tissue pigmentation, vascularity or indeed instrument setup, including illumination and camera parameters. Results of comprehensive ablation tests are to be reported in a separate publication. A sample of the augmented images using colour and contrast jitter is shown in figure 4.

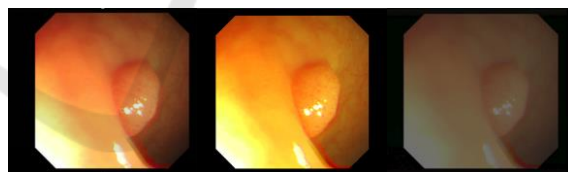


Figure 4: A sample of the augmented images using the colour and contrast jitter. From left: original, colour jitter and contrast jitter images.

4.2.2 Test-time Data Augmentation

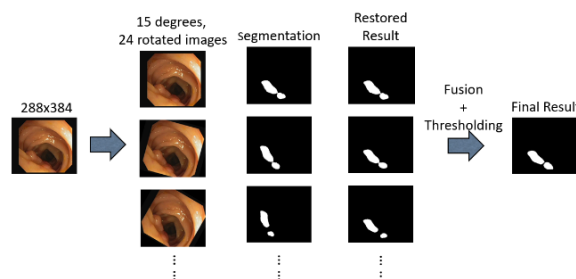


Figure 5: Test-time rotation based data augmentation.

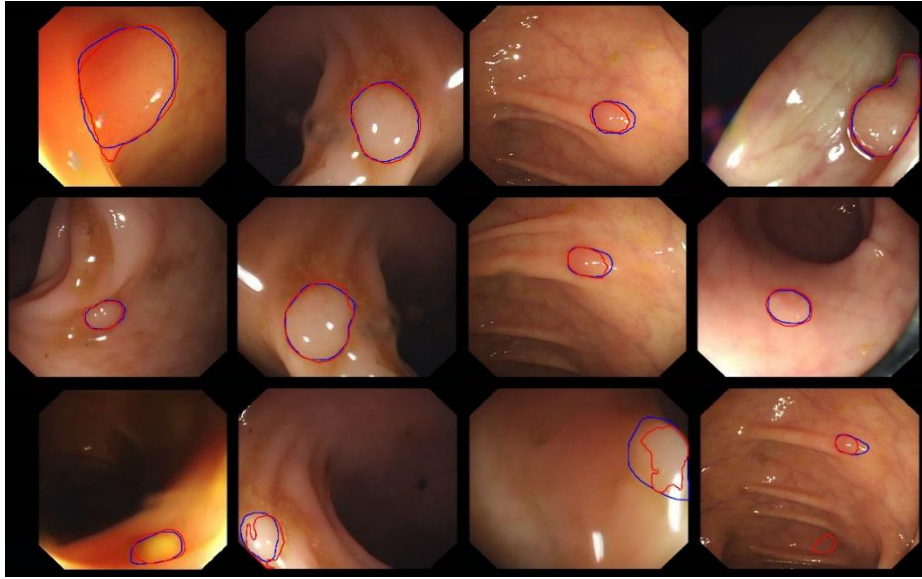


Figure 6: Typical results, with red and blue contours representing respectively segmentation results and the ground truth. Top: results obtained using the Dilated ResFCN network. Middle: results obtained using SE-Unet. Bottom: The segmented polyps using SE-Unet, which were not detected using the Dilated ResFCN.

Since the implemented CNNs don't have built in rotation invariance, one possible way to further improve the accuracy of the segmentation is to perform the rotation data augmentation during the test time. For this purpose rotated versions of the original test image are presented to the network and the corresponding outputs are averaged to better utilise generalisation capabilities of the network. The whole process is explained in figure 5. The test-time data augmentation implemented for the Dilated ResFCN uses 24 rotated images.

4.3 Evaluation Measures

4.3.1 Dice Index

For a single segmented polyp the Dice coefficient (also known as F1 score) is used as the base evaluation metric. It was also adopted as a metric by the GIANA challenge. This metric is used to compare the similarity between the binary segmentation results and the ground truth. It is calculated as follows:

$$Dice = \frac{2|S \cap G|}{|S| + |G|}$$

where: S represents the result of the segmentation, G represents the corresponding segmentation ground truth and |A| represent number of pixels in object A. As for the overall results obtained on the all test

images, the mean and the standard deviation of the Dice coefficients calculated for each image are used. Jaccard similarity index, also known as Intersection over Union, is another popular similarity metric often used in literature. However, as the Dice coefficient and Jaccard index have monotonic relation, only Dice coefficient results are reported in this paper.

4.3.2 Precision and Recall

Precision and recall are standard measures used in a context of binary classification. For image segmentation, precision is calculated as the ratio between the number of correctly segmented pixels and the number of all segmented pixels:

$$Precision = \frac{TP}{TP + FP}$$

Recall is calculated as a ratio between the number of the correctly segmented pixels and the number of pixels in the ground truth:

$$Recall = \frac{TP}{TP + FN}$$

In the context of image segmentation precision and recall could be used as indicators of over- and under-segmentation.

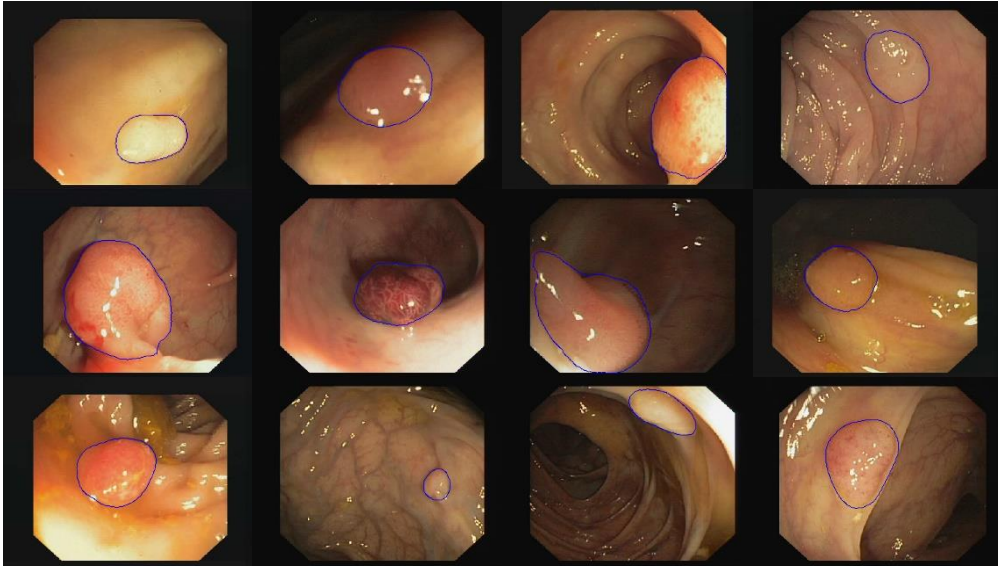


Figure 7: The typical segmentation results of a hybrid method for images form the test set.

4.3.3 Hausdorff Distance

In this work the Hausdorff distance is used to evaluate how closely the contour of the segmented polyp matches the shape of the corresponding ground truth. The Hausdorff distance is a common metric used to measure the similarity between contours of two objects. It is defined as:

$$\max\{sup_{x \in G} inf_{y \in S} d(x, y), sup_{x \in S} inf_{y \in G} d(x, y)\}$$

where: $d(x, y)$ denotes the distance between points $x \in G$ and $y \in S$. The smaller the value of the Hausdorff distance the better the two contours match, with the 0 indicating the perfect overlap between contours. It should be noted that the Hausdorff distance is complementary to the Dice coefficient as these metrics measure different properties of the segmented objects. It is quite possible to have segmentation results with the Dice coefficient close to 1 (with 1 indicating the perfect match) and the Hausdorff distance having a large value, indicating a poor contour match.

5 RESULTS

5.1 Validation Results

As part of selection of the design parameters the developed methods were tested on the 4-fold validation data (see section 4.1). A number of parameters have been tested, including parameters of

the backpropagation training algorithm (e.g. learning rate, momentum, number of epochs, etc.) or post processing such as polyp occurrence confidence map (POCM) threshold. This section shows only the results used to select which output of the Dilated ResFCN network should be used. The results from the proposed networks are also compared against the well-known FCN8 network (Long et al. 2015) and the hybrid method. The hybrid method uses the Dilated ResFCN as the base segmentation method and switches to the SE-Unet when the base network does not detect any polyp.

Table 1: Mean values obtained for different metrics on 4-fold validation data using FCN8s, Dilated ResFCN (DRFCN), SE-Unet and hybrid segmentation.

	Dice	Precision	Recall	Hausdorff
FCN8s Foreground	0.6321	0.6922	0.6497	271
FCN8s Background	0.6682	0.6767	0.6524	193
DRFCN Foreground	0.7789	0.8038	0.8099	56
DRFCN Background	0.7860	0.8136	0.8060	54
SE-Unet	0.6969	0.7477	0.7138	109
Hybrid	0.8014	0.8349	0.8210	62

Table 2: Statistics of the Dice coefficient obtained on the test data.

Method	Foreground			Background			Rotation test data augmentation		
	Mean	Std	Missing	Mean	Std	Missing	Mean	Std	Missing
Dilated ResFCN	0.7717	0.2394	17	0.8126	0.2043	9	0.8293	0.1956	9
SE-Usnet	0.8019	0.2240	14	N/A	N/A	N/A	0.8102	0.2207	13
Hybrid	0.7825	0.2204	6	0.8169	0.1904	6	0.8343	0.1837	3

As it can be seen from the Table 1 the overall best results are provided by the hybrid method followed by the Dilated ResFCN. Both proposed methods outperform the FCN8 segmentation network. A selection of typical results obtained on the validation data with different types of polyps is shown in Figure 6. This figure also demonstrates typical differences in the segmentation results generated by the two proposed methods.

5.2 Test Data Results

Table 2 shows the Dice coefficient’s mean and standard deviation as well as the number of missed polyps obtained on the test dataset. The results for the both proposed methods, and the hybrid method (see section 4.4) are shown. With the Dilated ResFCN used, the DICE segmentation statistics are reported when the foreground or the background network outputs are used. The results obtained with the test-time data augmentation are also reported. It can be seen that the best results, with biggest mean Dice coefficient, smallest Dice standard deviation and the smallest number of missed polyps are achieved by the hybrid method with implemented test-time data augmentation.

A sample of the typical segmentation results obtained by the hybrid method with the test-time data augmentation is shown in Figure 7. It should be noted that the method is able to successfully segment polyps of various size, shape and appearance. The Dilated ResFCN was used to generate results submitted to the GIANA 2017 challenge. The Dilated ResFCN clearly outperformed other submissions with the highest mean and the smallest standard deviation of the Dice coefficient. The results generated by the hybrid method with some added post processing (not reported in this paper) were submitted to the GIANA 2018 challenge. The submission secured second place, with small standard deviation and only slightly smaller Dice coefficient compared to the winning submission.

6 CONCLUSIONS

The paper describes two novel fully convolutional neural network architectures specifically designed for segmentation of polyps in video colonoscopy images. The networks have been developed and tested on the Gastrointestinal Image ANALysis – (GIANA) polyp segmentation database. The available training dataset with 300 low resolution and 56 high resolution images, is very limited from a perspective of a typical training set used in a context of the deep learning. Therefore, available data were heavily augmented with random rotation, translation, scale changes as well as colour and contrast jitter, with the rotation and colour jitter having the most significant effect on the quality of the segmentation. In total, after augmentation the training data include more than 90,000 images. The output from the network was optionally processed using the hybrid level set method. However, it should be noted that the DICE similarity scores obtained using a simple thresholding of the network outputs are very similar to the values of this measure obtained after applying the level set method. Nevertheless the level set could be used as it provides a simple mechanism to control smoothness of the segmented polyp boundaries. The proposed architectures provide competitive results, as is evident from the fact that they achieved the best results for the polyp segmentation task at the GIANA 2017 challenge and second place for polyp segmentation in the SD (low resolution) images at the GIANA 2018 challenge.

To the best knowledge of the authors, temporal dependencies in the colonoscopy video have not yet been used for polyp detection or segmentation within context of the deep architectures. The authors are aiming to examine various scenarios to test if such information could improve the overall performance of the polyp segmentation FCNNs. Two possible processing pipelines are to be investigated, with the explicit image warping obtained with a help of image registration (Shen et al., 2005) and implicit temporal fusion as part of the deep architecture.

ACKNOWLEDGEMENTS

The authors would like to acknowledge the organisers of the Gastrointestinal Image ANALysis – (GIANA) challenges for providing video colonoscopy polyp images.

REFERENCES

- Akbari, M., Mohrekesh, M., Nasr-Esfahani, E., Soroushmehr, S. M., Karimi, N., Samavi, S., & Najarian, K. (2018). Polyp Segmentation in Colonoscopy Images Using Fully Convolutional Network. *arXiv preprint arXiv:1802.00368*.
- Alexandre, L. A., Nobre, N., and Casteleiro, J. (2008). Color and position versus texture features for endoscopic polyp detection. In *BioMedical Engineering and Informatics, 2008. BMEI 2008. International Conference on* (Vol. 2, pp. 38-42). IEEE.
- Bernal, J., Sánchez, F. J., Fernández-Esparrach, G., Gil, D., Rodríguez, C., & Vilariño, F. (2015). WM-DOVA maps for accurate polyp highlighting in colonoscopy: Validation vs. saliency maps from physicians. *Computerized Medical Imaging and Graphics, 43*, 99-111.
- Bernal, J., Sánchez, J., & Vilarino, F. (2012). Towards automatic polyp detection with a polyp appearance model. *Pattern Recognition, 45*(9), 3166-3182.
- Bernal, J., Sánchez, J., & Vilarino, F. (2013). Impact of image preprocessing methods on polyp localization in colonoscopy frames. In *Engineering in Medicine and Biology Society (EMBC), 2013 35th Annual International Conference of the IEEE* (pp. 7350-7354). IEEE.
- Bernal, J., Tajkbaksh, N., Sánchez, F. J., Matuszewski, B. J., Chen, H., Yu, L., ... & Pogorelov, K. (2017). Comparative validation of polyp detection methods in video colonoscopy: results from the MICCAI 2015 Endoscopic Vision Challenge. *IEEE transactions on medical imaging, 36*(6), 1231-1249.
- Breier, M., Gross, S., and Behrens, A. (2011a). Chan-Vese-segmentation of polyps in colonoscopic image data. In *Proceedings of the 15th International Student Conference on Electrical Engineering POSTER* (Vol. 2011).
- Breier, M., Gross, S., Behrens, A., Stehle, T., and Aach, T. (2011b). Active contours for localizing polyps in colonoscopic nbi image data. In *Medical Imaging 2011: Computer-Aided Diagnosis* (Vol. 7963, p. 79632M). International Society for Optics and Photonics.
- Chen, L. C., Papandreou, G., Kokkinos, I., Murphy, K., and Yuille, A. L. (2018). Deeplab: Semantic image segmentation with deep convolutional nets, atrous convolution, and fully connected crfs. *IEEE transactions on pattern analysis and machine intelligence, 40*(4), 834-848.
- Glorot, X., and Bengio, Y. (2010). Understanding the difficulty of training deep feedforward neural networks. In *Proceedings of the thirteenth international conference on artificial intelligence and statistics* (pp. 249-256).
- Gross, S., Kennel, M., Stehle, T., Wulff, J., Tischendorf, J., Trautwein, C., and Aach, T. (2009). Polyp segmentation in NBI colonoscopy. In *Bildverarbeitung für die Medizin 2009* (pp. 252-256). Springer, Berlin, Heidelberg.
- Hernández-García, A., and König, P. (2018). Do deep nets really need weight decay and dropout?. *arXiv:1802.07042v3*
- He, K., Zhang, X., Ren, S., and Sun, J. (2016). Deep residual learning for image recognition. In *Proceedings of the IEEE conference on computer vision and pattern recognition* (pp. 770-778).
- Hu, J., Shen, L., and Sun, G. (2017). Squeeze-and-excitation networks. In *Proceedings of the IEEE Conference on Computer Vision and Pattern Recognition* (pp. 7132-7141).
- Hwang, S., Oh, J., Tavanapong, W., Wong, J., and De Groen, P. C. (2007). Polyp detection in colonoscopy video using elliptical shape feature. In *Image Processing, 2007. ICIP 2007. IEEE International Conference on* (Vol. 2, pp. II-465). IEEE.
- Iakovidis, D. K., Maroulis, D. E., Karkanis, S. A., and Brokos, A. (2005). A comparative study of texture features for the discrimination of gastric polyps in endoscopic video. In *Computer-Based Medical Systems, 2005. Proceedings. 18th IEEE Symposium on* (pp. 575-580). IEEE.
- Karkanis, S. A., Iakovidis, D. K., Maroulis, D. E., Karras, D. A., and Tzivras, M. (2003). Computer-aided tumor detection in endoscopic video using color wavelet features. *IEEE transactions on information technology in biomedicine, 7*(3), 141-152.
- Krizhevsky, A., Sutskever, I., and Hinton, G. E. (2012). Imagenet classification with deep convolutional neural networks. In *Advances in neural information processing systems* (pp. 1097-1105).
- LeCun, Y., Bottou, L., Bengio, Y., and Haffner, P. (1998). Gradient-based learning applied to document recognition. *Proceedings of the IEEE, 86*(11), 2278-2324.
- Li, Q., Yang, G., Chen, Z., Huang, B., Chen, L., Xu, D., ... and Wang, T. (2017). Colorectal polyp segmentation using a fully convolutional neural network. In *Image and Signal Processing, BioMedical Engineering and Informatics (CISP-BMEI), 2017 10th International Congress on* (pp. 1-5). IEEE.
- Long, J., Shelhamer, E., and Darrell, T. (2015). Fully convolutional networks for semantic segmentation. In *Proceedings of the IEEE conference on computer vision and pattern recognition* (pp. 3431-3440).
- Park, S., Lee, M., and Kwak, N. (2015). Polyp detection in colonoscopy videos using deeply-learned hierarchical features. *Seoul National University*.

- Peng, C., Zhang, X., Yu, G., Luo, G., and Sun, J. (2017). Large kernel matters—improve semantic segmentation by global convolutional network. In *Computer Vision and Pattern Recognition (CVPR), 2017 IEEE Conference on* (pp. 1743-1751). IEEE.
- Ribeiro, E., Uhl, A., and Häfner, M. (2016). Colonic polyp classification with convolutional neural networks. In *Computer-Based Medical Systems (CBMS), 2016 IEEE 29th International Symposium on* (pp. 253-258). IEEE.
- Ronneberger, O., Fischer, P., and Brox, T. (2015). U-net: Convolutional networks for biomedical image segmentation. In *International Conference on Medical image computing and computer-assisted intervention* (pp. 234-241). Springer, Cham.
- Shen, J. K., Matuszewski, B. J., and Shark, L. K. (2005). Deformable image registration. In *Image Processing, 2005. ICIP 2005. IEEE International Conference on* (Vol. 3, pp. III-1112). IEEE.
- Tajbakhsh, N., Chi, C., Gurudu, S. R., and Liang, J. (2014a). Automatic polyp detection from learned boundaries. In *Biomedical Imaging (ISBI), 2014 IEEE 11th International Symposium on* (pp. 97-100). IEEE.
- Tajbakhsh, N., Gurudu, S. R., and Liang, J. (2013). A classification-enhanced vote accumulation scheme for detecting colonic polyps. In *International MICCAI Workshop on Computational and Clinical Challenges in Abdominal Imaging* (pp. 53-62). Springer, Berlin, Heidelberg.
- Tajbakhsh, N., Gurudu, S. R., and Liang, J. (2014b). Automatic polyp detection using global geometric constraints and local intensity variation patterns. In *International Conference on Medical Image Computing and Computer-Assisted Intervention* (pp. 179-187). Springer, Cham.
- Vázquez, D., Bernal, J., Sánchez, F. J., Fernández-Esparrach, G., López, A. M., Romero, A., ... and Courville, A. (2017). A benchmark for endoluminal scene segmentation of colonoscopy images. *Journal of healthcare engineering, 2017*.
- Yu, F., and Koltun, V. (2015). Multi-scale context aggregation by dilated convolutions. *arXiv preprint arXiv:1511.07122*.
- Zhang, L., Dolwani, S., and Ye, X. (2017). Automated polyp segmentation in colonoscopy frames using fully convolutional neural network and textons. In *Annual Conference on Medical Image Understanding and Analysis* (pp. 707-717). Springer, Cham.
- Zhang, R., Zheng, Y., Mak, T. W. C., Yu, R., Wong, S. H., Lau, J. Y., and Poon, C. C. (2017). Automatic Detection and Classification of Colorectal Polyps by Transferring Low-Level CNN Features From Nonmedical Domain. *IEEE J. Biomedical and Health Informatics, 21*(1), 41-47.
- Zhang, Y., and Matuszewski, B. J. (2009). Multiphase active contour segmentation constrained by evolving medial axes. In *Image Processing (ICIP), 2009 16th IEEE International Conference on* (pp. 2993-2996). IEEE.
- Zhang, Y., Matuszewski, B. J., Shark, L. K., and Moore, C. J. (2008). Medical image segmentation using new hybrid level-set method. In *Fifth International Conference BioMedical Visualization: Information Visualization in Medical and Biomedical Informatics* (pp. 71-76). IEEE.